Electronic Supplementary Material (ESI) for Journal of Materials Chemistry C.

Supporting Information

A Ternary Organic Solar Cell with 15.6% Efficiency Containing a New DPP-based Acceptor

María Privado,[1] Hemraj Dahiya,[2] Pilar de la Cruz,[1] Mukhamed L. Keshtov,[3] Fernando Langa,*[1] and Ganesh D. Sharma*[2]*

[1] Universidad de Castilla-La Mancha, Instituto de Nanociencia, Nanotecnología and Materiales Moleculares (INAMOL), Campus de la Fábrica de Armas, 45071-Toledo, Spain. E-mail: Fernando.Langa@uclm.es

[2] Department of Physics, The LNM Institute of Information Technology (Deemed University), Jamdoli, Jaipur (Raj.) 302031, India. E-mail: gdsharma@lnmiit.ac.in

[3] A. N. Nesmeyanov Institute of Organoelement Compounds of the Russian Academy of Sciences, Vavilova St., 28, 119991, Moscow, Russian Federation

1. General Remarks.

Experimental conditions. Anhydrous solvents were dried by purification system Pure-Sov 400. Chromatographic purifications were performed using silica gel 60 Merk 230-400 mesh ASTM. Analytical thin-layer chromatography was performed using ALUGRAM ® SIL G/UV_{254} silica gel 60. Nuclear magnetic resonance ^{1}H NMR and ^{13}C NMR were performed using Bruker Innova 400 Hz. Chemical shifts (δ) values are denoted in ppm. Residual solvent peaks being used as the internal standard ($CHCl_3$; $\delta = 7.27$ ppm). ^{13}C NMR chemical shifts are reported relative to the solvent residual peaks ($CDCl_3$, $\delta = 77.00$ ppm). MALDI-TOF spectra were obtained in VOYAGER DETM STR spectrometry, using Dithranol [1,8-dihydroxy-9(10H)-anthracenone] as matrix. Fourier transform infrared spectrophotometer (FT-IR) Thermo Nicolet AVATAR 370 was used with KBr method; in each case the most characteristic bands are indicated for each compound. Absorption spectra were performed on Shimadzu UV 3600 spectrophotometer. Solutions of different concentration were prepared in CH_2Cl_2, spectroscopy grade, with absorbance between 0.5 and 0.7 using a 1 cm UV cuvette. Thermogravimetric analyses were performed using a TGA/DSC Linea Excellent instrument by Mettler-Toledo and collected under inert atmosphere of nitrogen with a scan rate of 10 °C min^{-1}. The weight changes were recorded as a function of temperature.

Electrochemical Measurements: Reduction (E_{red}) and oxidation potentials (E_{ox}) were measured by cyclic voltammetry with a potentiostat BAS CV50W in a conventional three-electrode cell equipped with a glassy carbon working electrode, a platinum wire counter electrode, and an $Ag/AgNO_3$ reference electrode at scan rate of 100 mV/s. The E_{red} and E_{ox} were expressed vs. Fc/Fc^+ used as external reference. In each case, the measurements were done in a deaerated solution containing 1 mM of a the sample compound in 0.1 M of $(n\text{-}Bu)_4NClO_4$ in *o*-DCB:Acetonitrile (4:1) as an electrolyte solution.

Computational Details: Theoretical calculations were carried out within the density functional theory (DFT) framework by using the Gaussian 09, applying density functional theory at the B3LYP level. The basis set of 6-31G* was used in the calculations (Supercomputation Service of UCLM).

2. Synthesis and characterization of compound 2, 3, 5 and MPU6.

Synthesis of compound 2: Under argon atmosphere, over a stirred solution of compound **1** (0.49 mmol, 384 mg), $Pd(PPh_3)_4$ (0.02 mmol, 28.6 mg) and CuI (0.05 mmol, 9.4 mg) in 11.6 mL of anhydrous triethylamine was added ethynyltrimethylsilane (2.5 mmol, 246.9 mg) and the mixture was stirred overnight at room temperature. Then, the reaction was quenched with a saturated solution of NH_4Cl and extracted several times with CH_2Cl_2. The organic phase was dried with Na_2SO_4 and the solvent was removed under reduced pressure. The crude was purified by washing three times with methanol to obtain compound **2** as a solid product (382 mg, 96 %).

^{1}H NMR (400 MHz, $CDCl_3$) δ/ppm: 8.75 (d, *J* = 4.3 Hz, 2H), 7.50 (d, *J* = 4.3 Hz, 2H), 3.94 (m, 4H), 1.88 (s, 2H), 1.31 (m, 16H), 0.88 (m, 12H), 0.28 (s, 18H). **^{13}C NMR** (100 MHz, $CDCl_3$) δ/ppm: 161.5, 139.6, 135.3, 133.6, 130.4, 128.3, 108.9, 104.2, 96.6, 46.0, 39.0, 30.1, 28.3, 23.5, 23.0, 14.0, 10.4, 0. **MALDI-TOF MS** (*m/z*): calculated 812.2 $[M]^+$ for $C_{40}H_{56}N_2O_2Se_2Si_2$; found 813.068 $[M+1]^+$.

Synthesis of compound 3: Under argon atmosphere, KF (1.85 mmol, 107 mg) was added over a solution of compound **2** (0.18 mmol, 150 mg) in a mixed of 7.4 mL of THF/water 7:2 and stirred at room temperature overnight. The reaction mixture was quenched with water and extracted three times with CH_2Cl_2. The organic phase was dried with Na_2SO_4 and the solvent was removed under reduced pressure. The crude was purified by washing with methanol and hexane to obtain a purple solid (115 mg, 96 %).

^{1}H NMR (400 MHz, $CDCl_3$) δ/ppm: 8.76 (d, J = 4.0 Hz, 2H), 7.57 (d, J = 4.0 Hz, 2H), 3.95 (m, 4H), 3.81 (m, 2H), 1.93 – 1.82 (m, 4H), 1.29 (m, 16H), 0.88 (m, 12H). **^{13}C NMR** (100 MHz, $CDCl_3$) δ/ppm: 161.6, 141.4, 136.4, 136.3, 135.4, 132.5, 109.0, 87.7, 78.5, 46.0, 39.1, 30.1, 29.7, 28.2, 23.5, 23.1, 14.0, 10.4. **MALDI-TOF MS** (*m/z*): calculated 668.1 $[M]^+$ for $C_{34}H_{40}N_2O_2Se_2$; found 669.059 $[M+1]^+$.

Synthesis of compound 5: Under argon atmosphere, 3,4-dihexyl-5-iodothiophene-2-carbaldehyde[1] (**4**) (0.44 mmol, 179 mg) and 7.6 mL of triethylamine were added over a stirred solution of compound **3** (0.17 mmol, 113 mg), $AsPh_3$ (0.68 mmol, 207 mg) and $Pd_2(dBa)_3$ (0.10 mmol, 93 mg) in 32 mL of anhydrous THF and the reaction mixture was warmed at reflux overnight. After cooling, the solution was quenched with water and extracted several times with CH_2Cl_2. The organic phase was dried over anhydrous Na_2SO_4, and the solvent was removed under reduced pressure; the obtained solid was purified by column chromatography (silica gel, 4:6 *n*-hexane/ CH_2Cl_2) to afford a blue powder (74 mg, 39 %).

[1] Arrechea, S.; Molina-Ontoria, A.; Aljarilla, A.; de la Cruz, P.; Langa, F.; Echegoyen, L. *Dye. Pigment.* **2015**, *121*, 109.

^{1}H NMR (400 MHz, $CDCl_3$) δ/ppm: 10.01 (s, 2H), 8.84 (d, *J* = 3.8 Hz, 2H), 7.58 (d, *J* = 3.8 Hz, 2H), 3.97 (m, 4H), 2.90 (t, *J* = 8 Hz, 4H), 2.71 (t, *J* = 8 Hz, 4H), 1.90 (m, 2H), 1.59 (m, 12H), 1.48-1.17 (m, 36H), 0.90 (m, 24H); **^{13}C NMR** (100 MHz, $CDCl_3$) δ/ppm: 182.1, 161.6, 151.2, 149.3, 141.2, 138.6, 136.2, 135.7, 132.4, 127.1, 109.4, 94.2, 92.9, 46.1, 39.1, 32.2, 31.6, 31.5, 30.2, 29.7, 29.3, 28.3, 28.1, 27.3, 23.1, 22.6, 22.5, 14.1, 14.0, 14.0, 10.5; **MALDI-TOF MS** (m/z): calculated 1224.48 $[M]^+$ for $C_{68}H_{92}N_2O_4S_2Se_2$; found 1224.286 $[M]^+$.

Synthesis of MPU6: Under argon atmosphere, ammonium acetate (0.25 mmol, 19.3 mg) was added over a stirred solution of compound **5** (0.05 mmol, 63 mg) and 2-(1,1-dicyanomethylene)-3-ethylrhodanine[2] (**6**) (0.15 mmol, 29 mg) in 3 mL of glacial acetic acid and the reaction mixture was reflux overnight; then, the mixture was cooled and poured over ice water. The crude was extracted three times with $CHCl_3$. The organic phase was washed with $NaHCO_3$, dried with Na_2SO_4 and the solvent was removed under reduced pressure. The crude was purified by flash chromatography column (silica gel, *n*-hexane: $CHCl_3$: acetone 8:2:1) and washed with ethanol and hexane to obtain the desired product **MPU6** as a greenish brown solid (53 mg, 67 %).

^{1}H-NMR (400 MHz, $CDCl_3$) δ/ppm: 8.89 (d, *J* = 4.4 Hz, 2H), 8.11 (s, 2H), 7.60 (d, *J* = 4.4 Hz, 2H), 4.34 (m, 4H), 3.98 (m, 4H), 2.74 (m, 8H), 1.91 (s, 2H), 1.66 – 1.48 (m, 12H), 1.45 – 1.26 (m, 42H), 0.90 (m, 24H). **^{13}C-NMR** (100 MHz, $CDCl_3$) δ/ppm: 165.9, 165.2, 161.6, 150.0, 149.3, 141.2, 137.0, 136.4, 135.9, 133.3, 132.2, 126.9, 126.2, 114.3, 113.1, 112.3, 109.4, 96.3, 92.8, 55.9, 46.1, 40.1, 39.1, 31.8, 31.5, 30.1, 29.3, 29.2, 28.6, 28.3, 27.8, 23.6, 23.1, 22.6, 22.5, 14.2, 14.1, 14.0, 10.5. **FT-IR** (KBr) ν/ cm^{-1}: 2956.7, 2925.8, 2856.3, 2214.9, 1720.4, 1666.4, 1573.66, 1542.7, 1450.0, 1202.8, 1133.2. **MS** (MALDI-TOF) (m/z): calculated 1574.52 $[M+H]^+$ for $C_{84}H_{102}N_4O_4S_4Se_2$; found 1574.994 $[M]^+$.

[2] Zhang, Q.; Kan, B.; Liu, F.; Long, G.; Wan, X.; Chen, X.; Zuo, Y.; Ni, W.; Zhang, H.; Li, M.; Hu, Z.; Huang, F.; Cao, Y.; Liang, Z.; Zhang, M.; Russell, T. P.; Chen, Y. *Nat Phot.* **2015**, *9* (1), 35.

3. ^{1}H NMR, ^{13}C NMR, FT-IR and MALDI-TOF spectra.

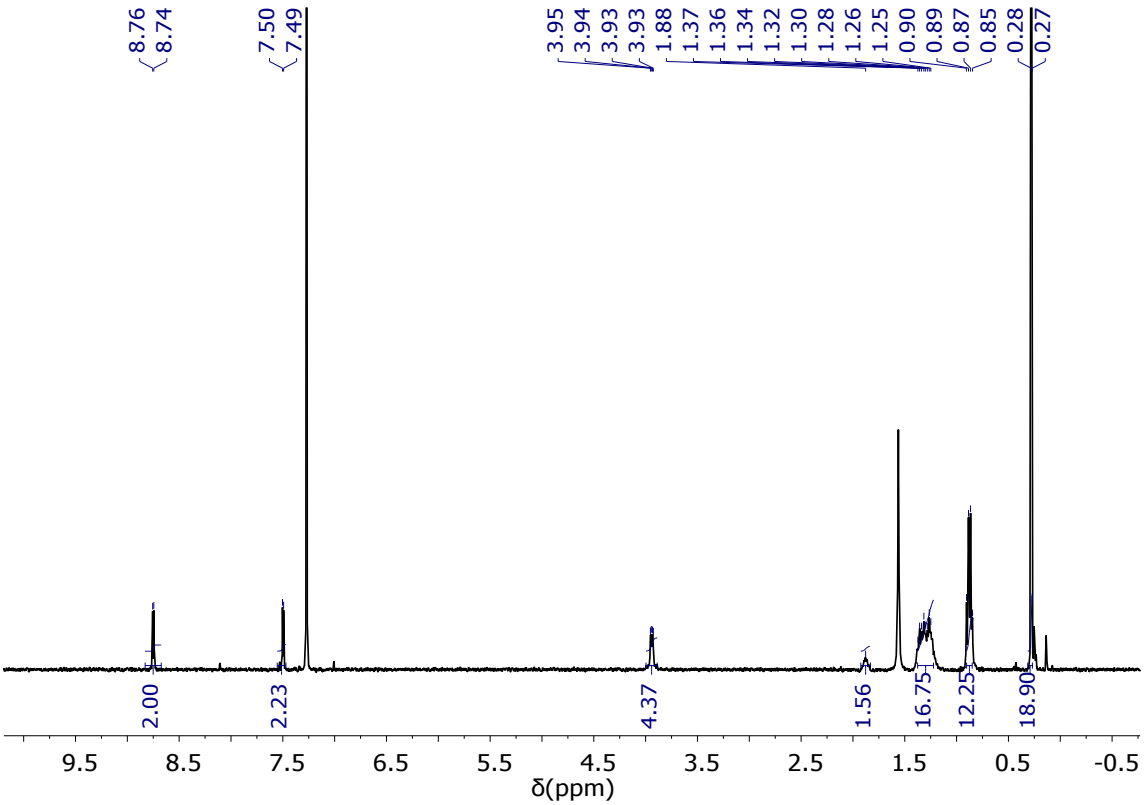

Figure S1. ^{1}H-NMR (400MHz, $CDCl_3$) spectrum of Compound **2.**

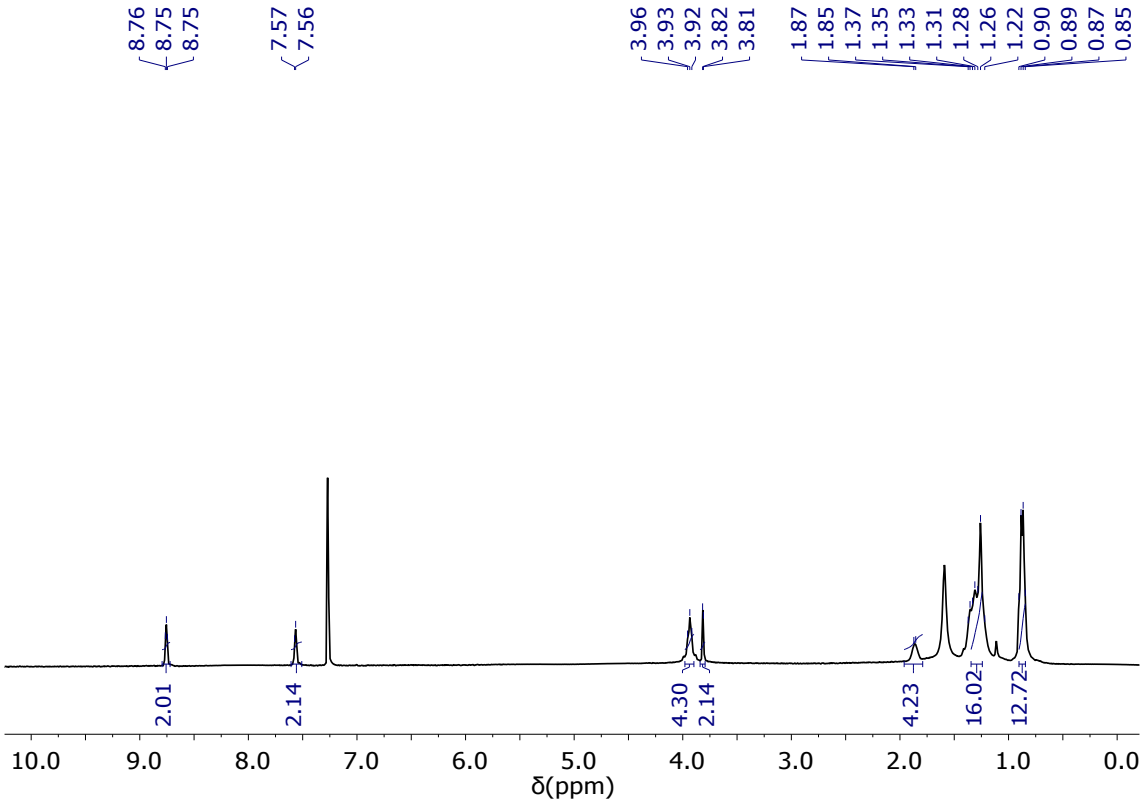

Figure S2. ^{1}H-NMR (400MHz, $CDCl_3$) spectrum of Compound **3.**

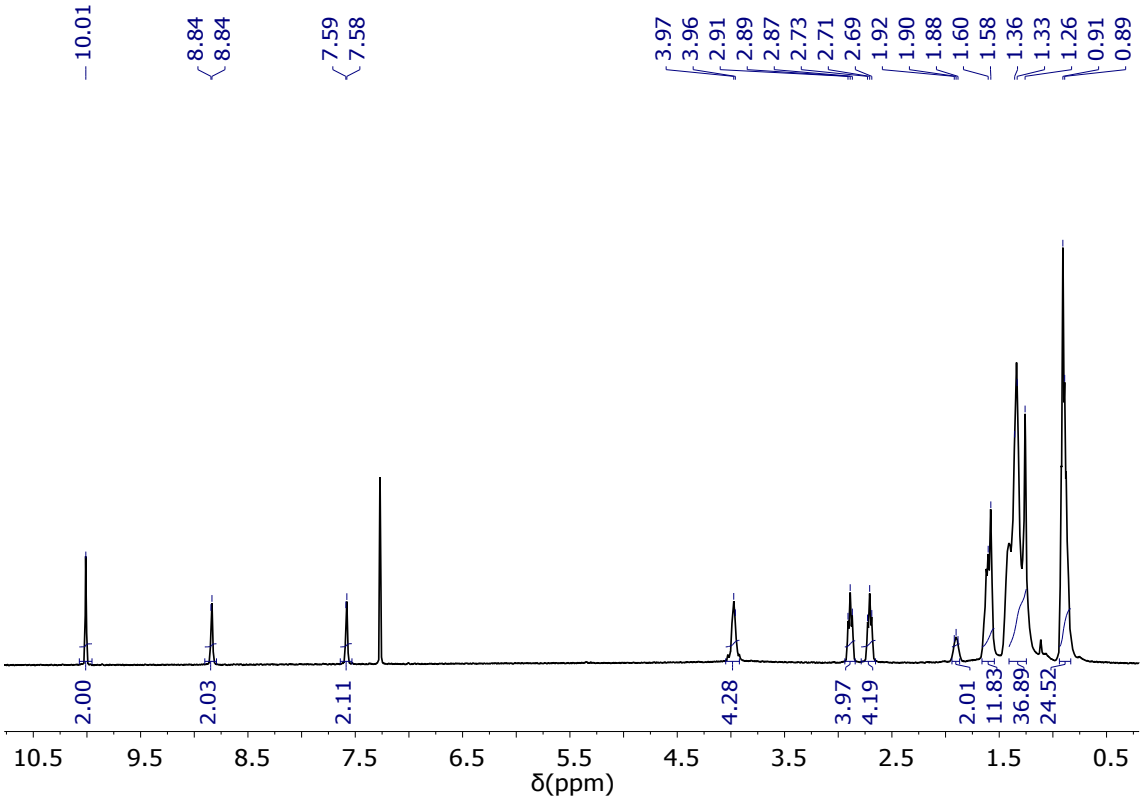

Figure S3. ^{1}H-NMR (400MHz, $CDCl_3$) spectrum of Compound **5.**

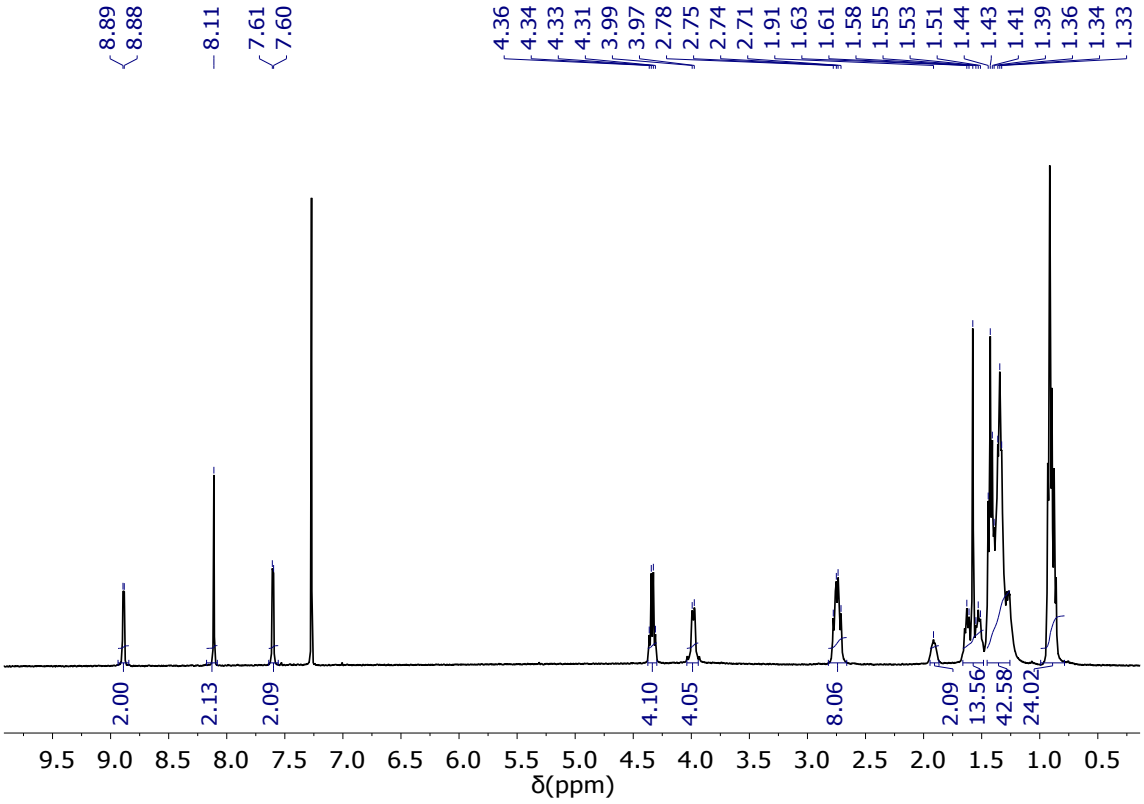

Figure S4. ^{1}H-NMR (400MHz, $CDCl_3$) spectrum of **MPU6.**

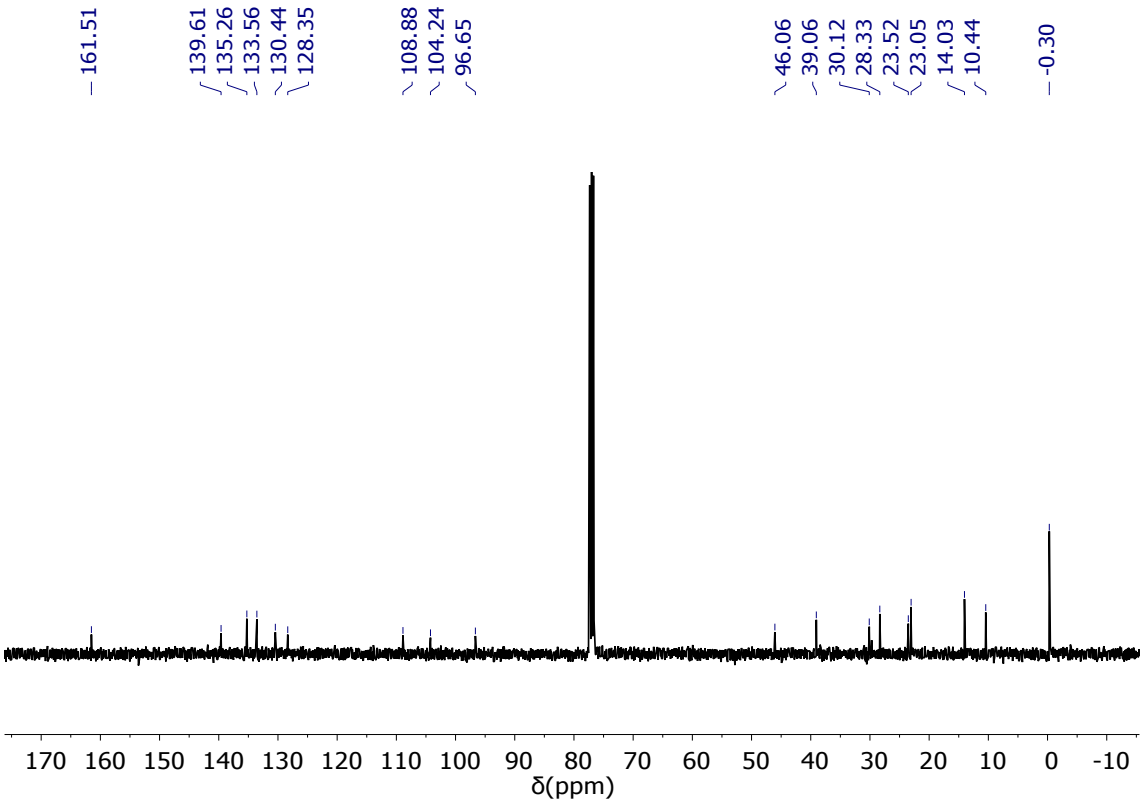

Figure S5. ^{13}C-NMR (100MHz, $CDCl_3$) spectrum of Compound **2.**

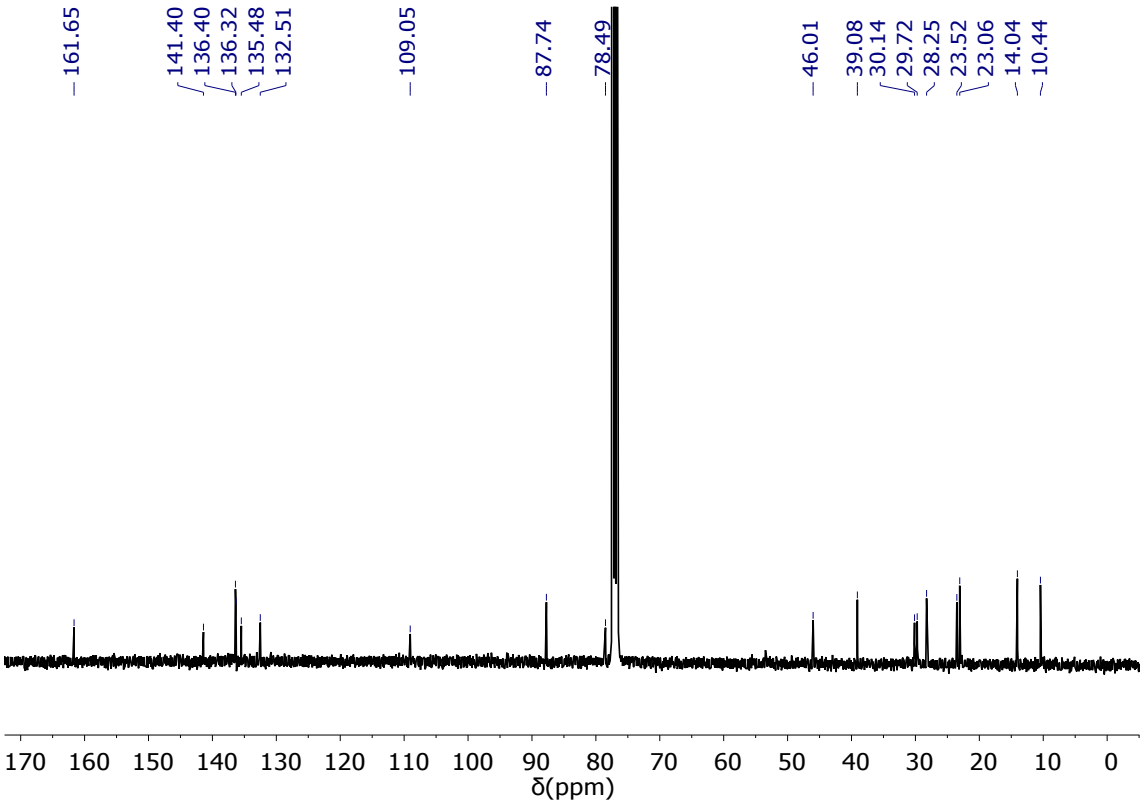

Figure S6. ^{1}H-NMR (400MHz, $CDCl_3$) spectrum of Compound **3.**

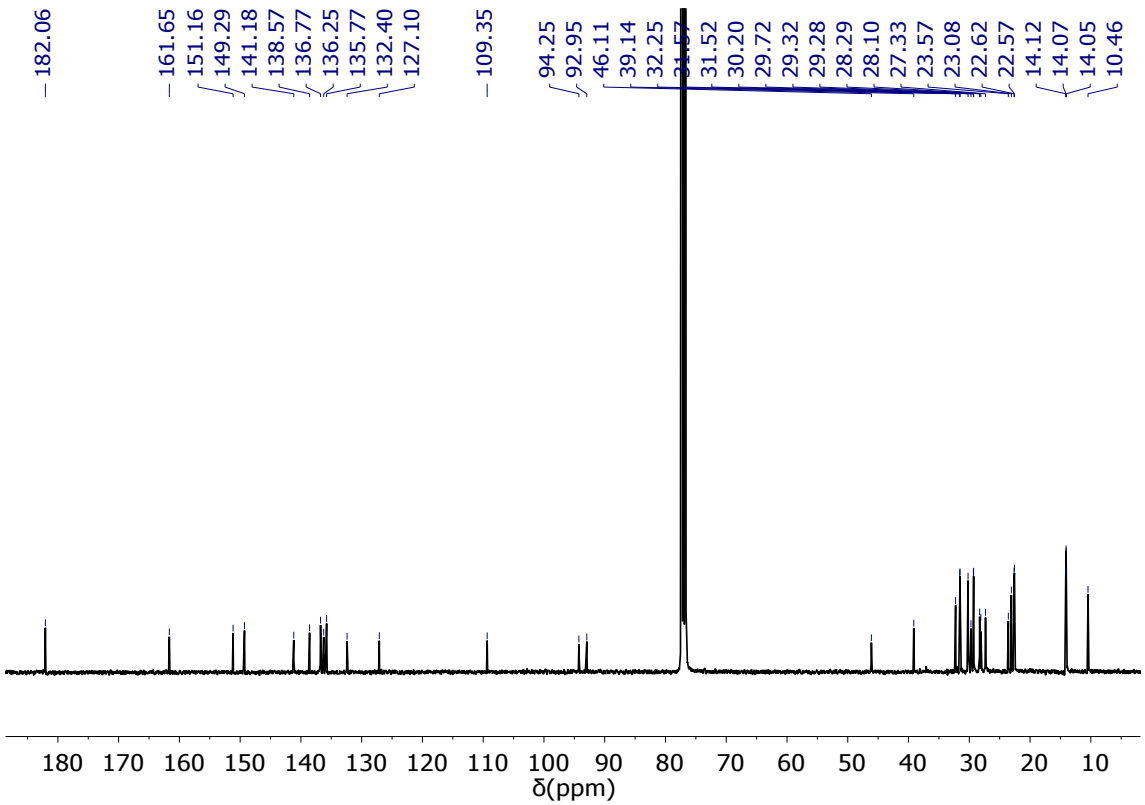

Figure S7. ^{13}C-NMR (100MHz, $CDCl_3$) spectrum of compound **5.**

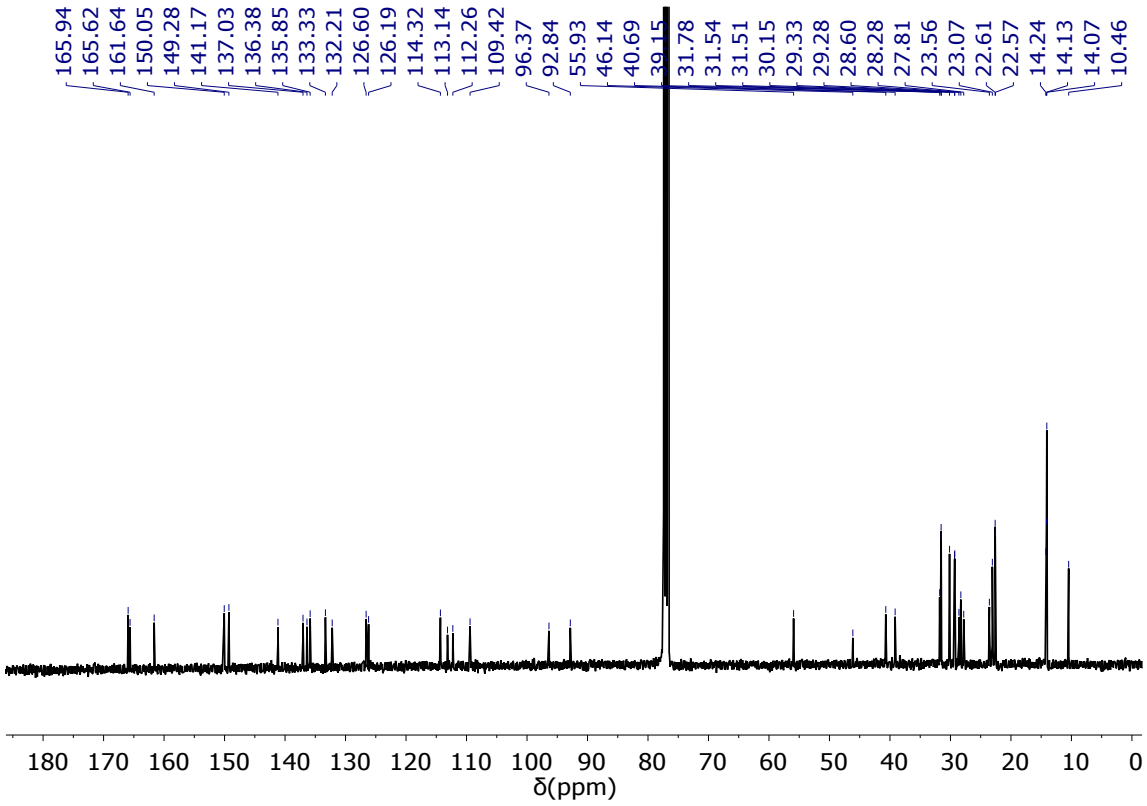

Figure S8. ^{13}C-NMR (100MHz, $CDCl_3$) spectrum of **MPU6.**

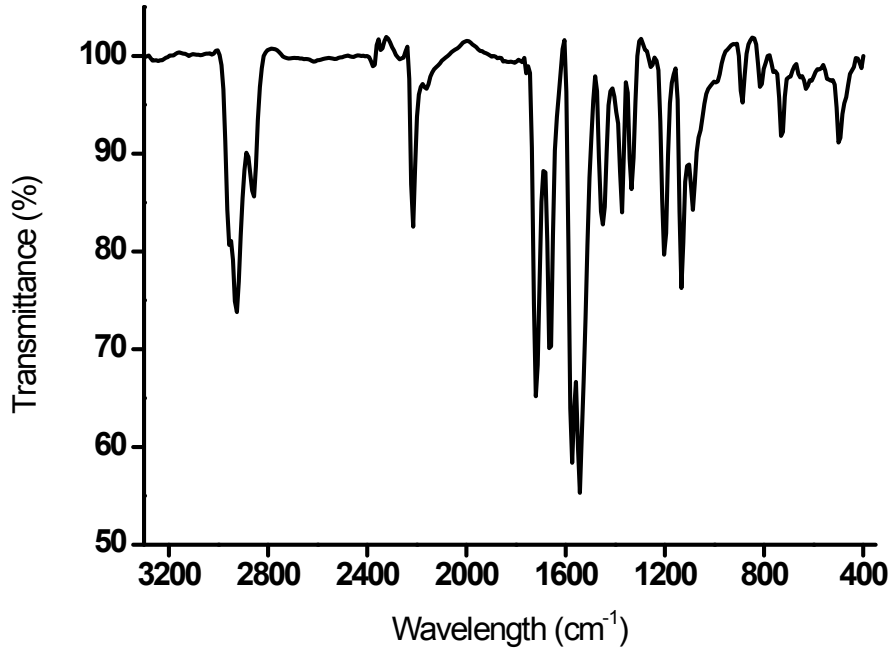

Figure S9. FT-IR (KBr) spectrum of **MPU6**.

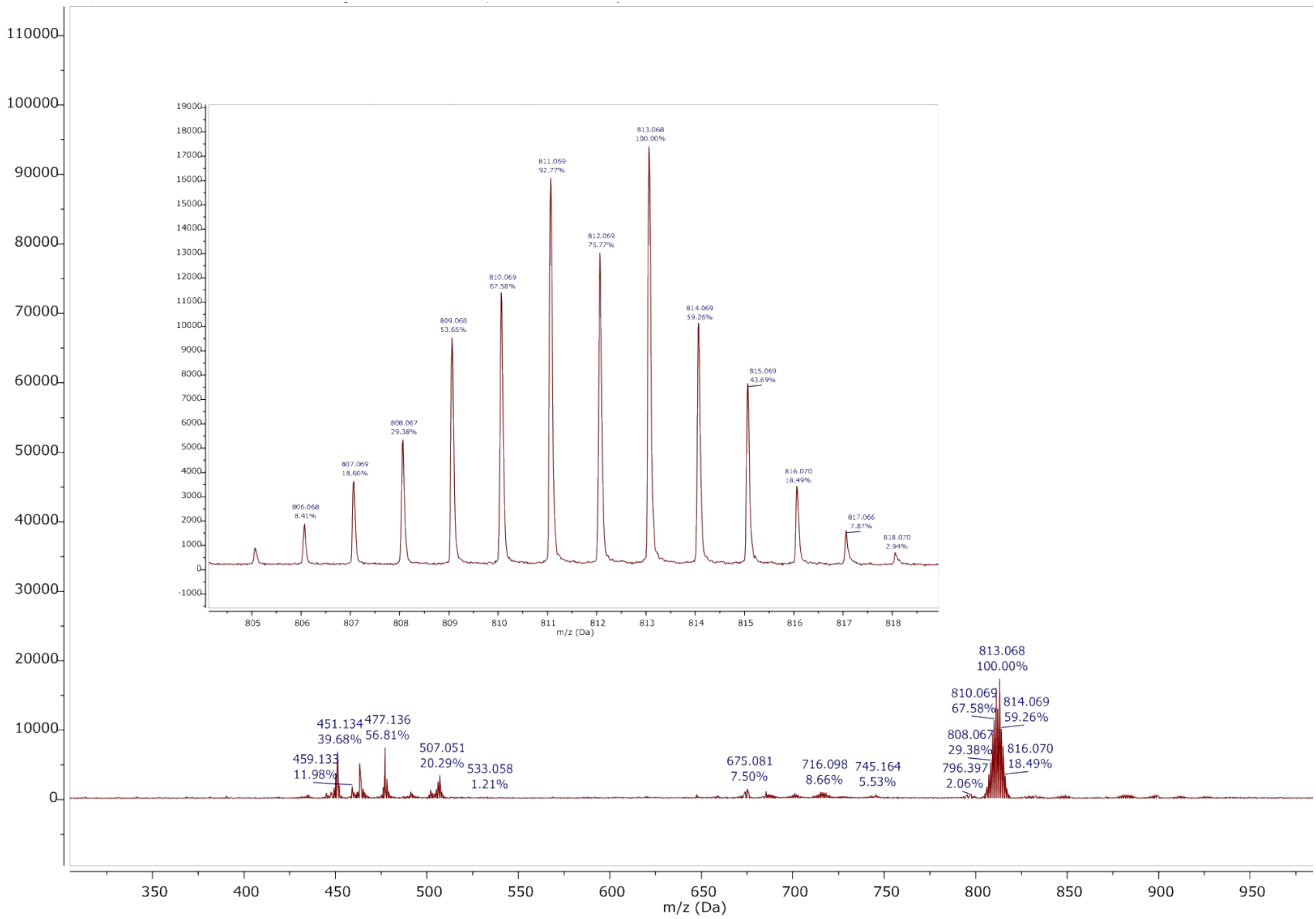

Figure S10. MALDI-TOF MS spectrum of compound **2** (Matrix: Dithranol).

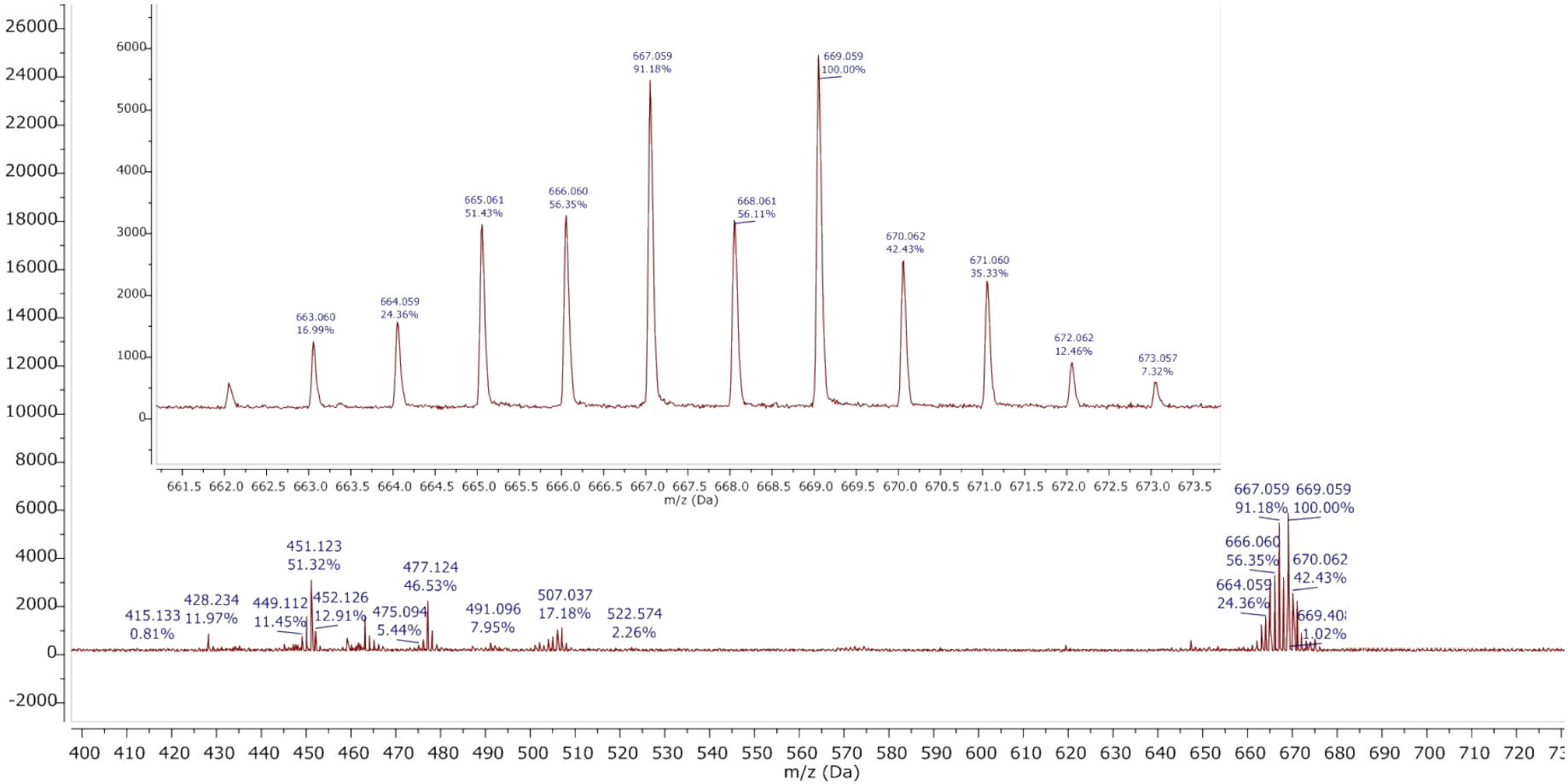

Figure S11. MALDI-TOF MS spectrum of compound **3** (Matrix: Dithranol).

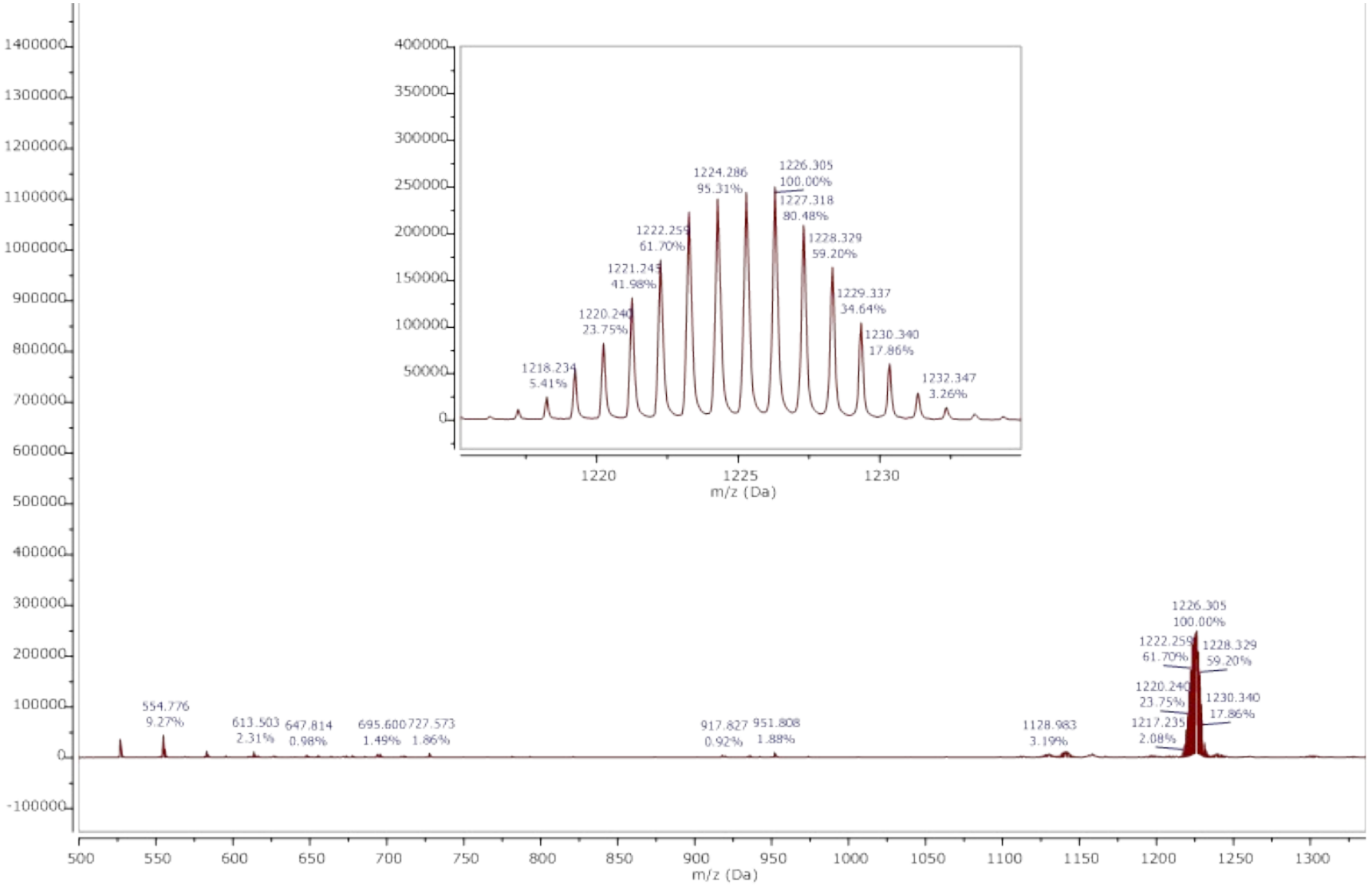

Figure S12. MALDI-TOF MS spectrum of compound **5** (Matrix: Dithranol).

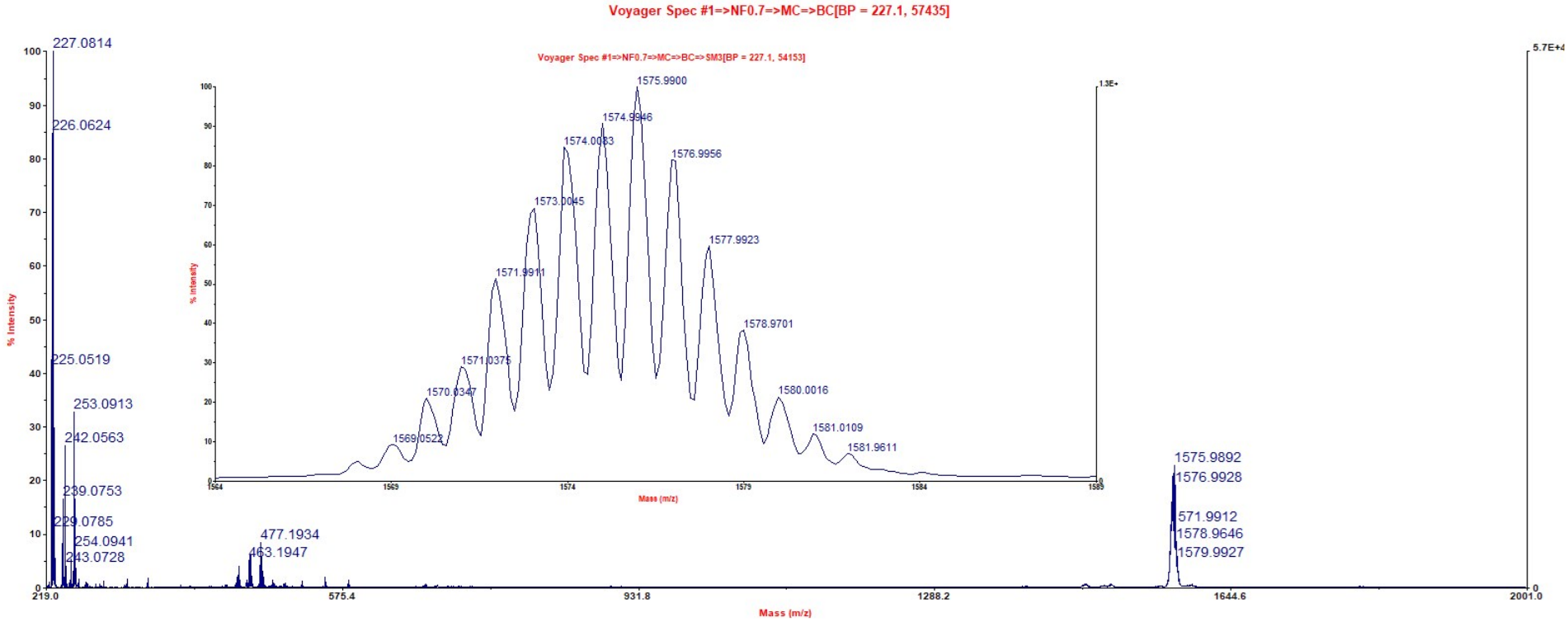

Figure S13. MALDI-TOF MS spectrum of **MPU6** (Matrix: Dithranol).

4. Thermogravimetric Analysis (TGA) and Differential Scanning Calorimetry (DSC) of MPU6.

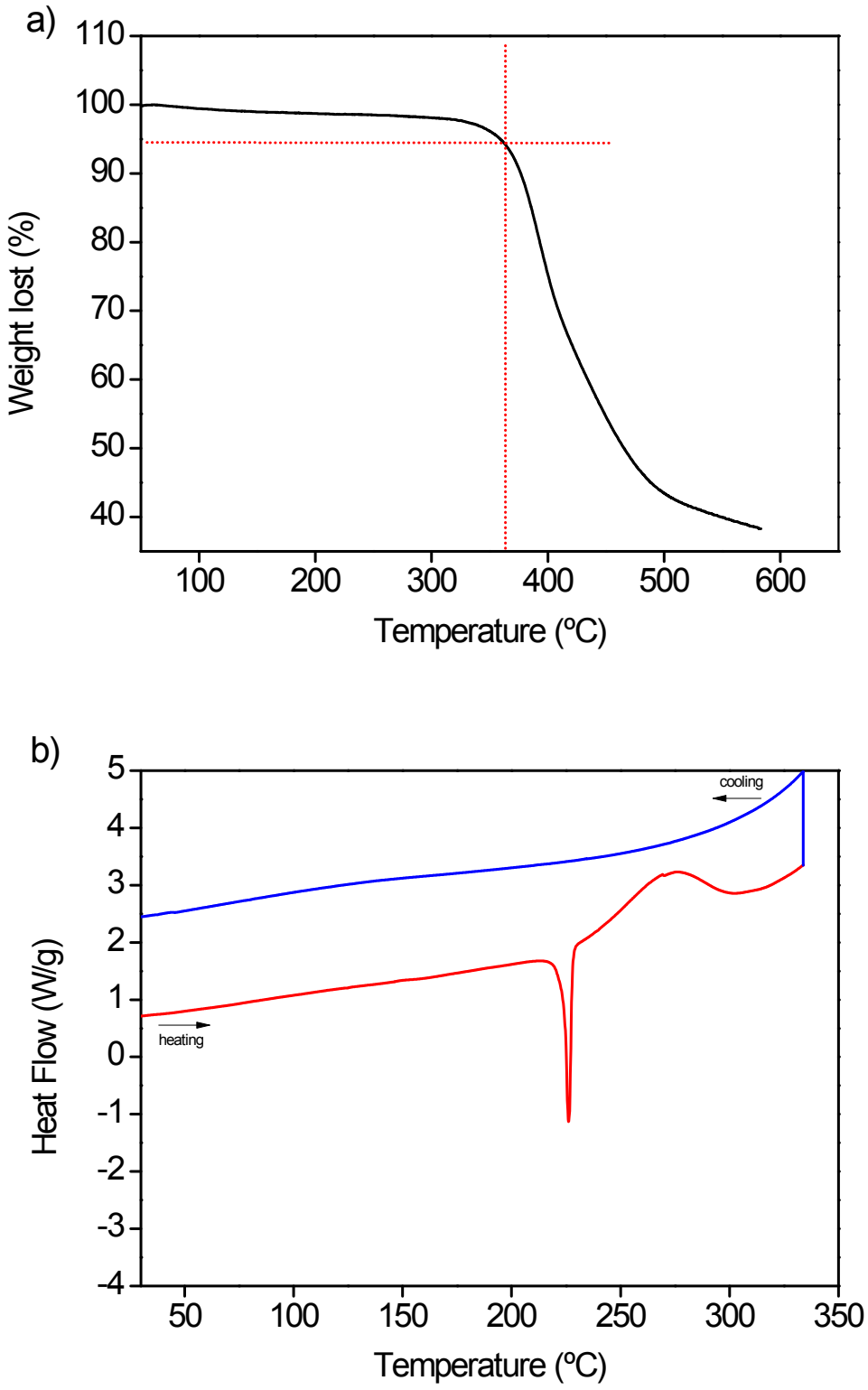

Figure S14. a) TGA and b) DSC curves of **MPU6**.

5. Theoretical calculations

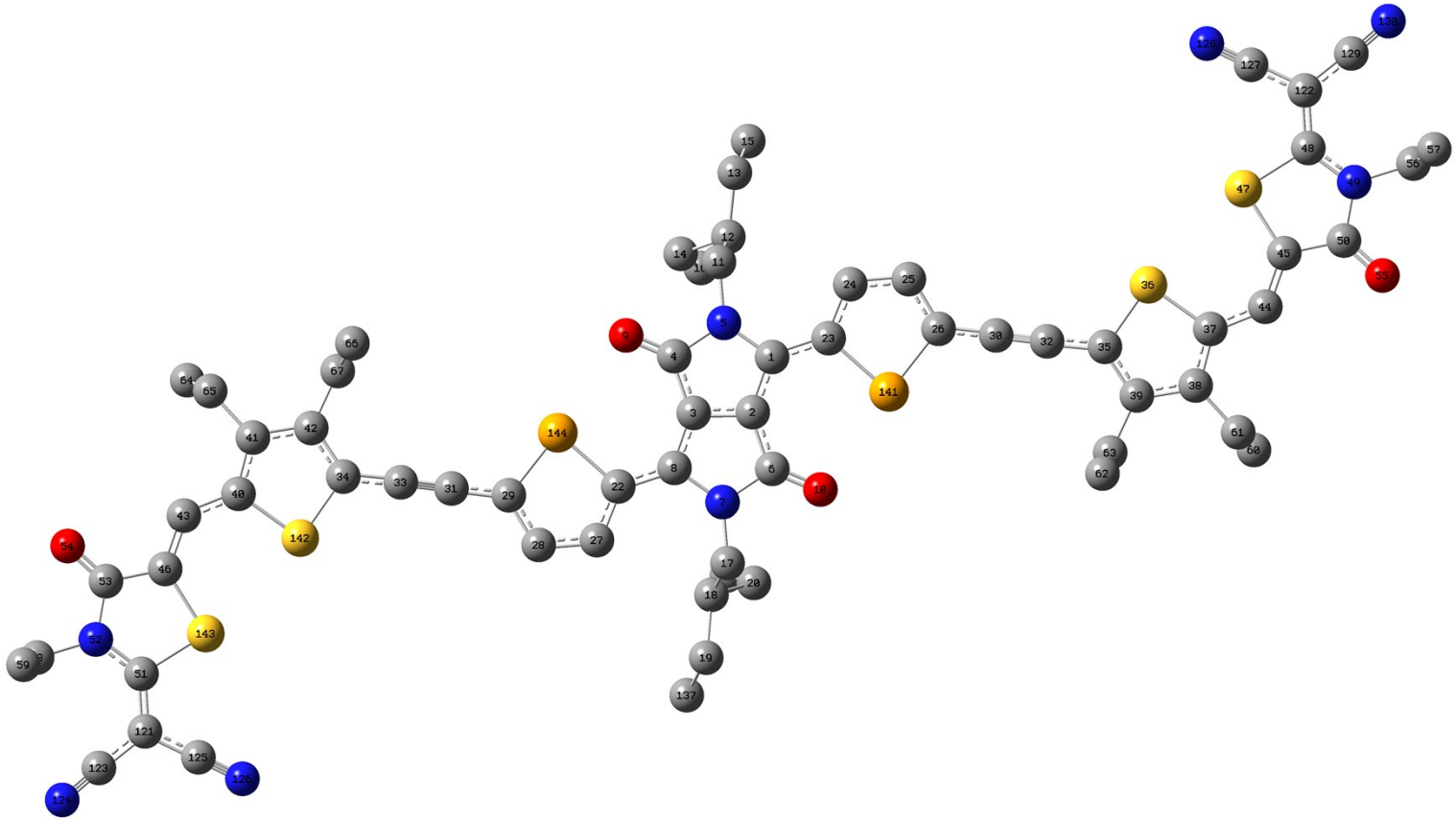

Figure S15. Theoretical structure of **MPU6** with atom labels.

Optimized Parameters (Angstroms and Degrees)			
Name	Definition	Value	Derivative Info.
R1	R(1,2)	1.4015	-DE/DX = 0.0
R2	R(1,5)	1.4132	-DE/DX = 0.0
R3	R(1,23)	1.4286	-DE/DX = 0.0
R4	R(2,3)	1.4173	-DE/DX = 0.0
R5	R(2,6)	1.4368	-DE/DX = 0.0
R6	R(3,4)	1.4368	-DE/DX = 0.0
R7	R(3,8)	1.4015	-DE/DX = 0.0
R8	R(4,5)	1.4374	-DE/DX = 0.0
R9	R(4,9)	1.2557	-DE/DX = 0.0
R10	R(5,11)	1.468	-DE/DX = 0.0
R11	R(6,7)	1.4374	-DE/DX = 0.0
R12	R(6,10)	1.2557	-DE/DX = 0.0
R13	R(7,8)	1.4132	-DE/DX = 0.0
R14	R(7,17)	1.468	-DE/DX = 0.0
R15	R(8,22)	1.4286	-DE/DX = 0.0
R16	R(11,12)	1.5523	-DE/DX = 0.0
R17	R(11,68)	1.0948	-DE/DX = 0.0
R18	R(11,69)	1.0948	-DE/DX = 0.0
R19	R(12,13)	1.5502	-DE/DX = 0.0
R20	R(12,14)	1.5573	-DE/DX = 0.0
R21	R(12,70)	1.1001	-DE/DX = 0.0
R22	R(13,15)	1.5365	-DE/DX = 0.0
R23	R(13,71)	1.1007	-DE/DX = 0.0

```
 ! R24   R(13,72)                1.1014          -DE/DX =    0.0
!
 ! R25   R(14,16)                1.5389          -DE/DX =    0.0
!
 ! R26   R(14,73)                1.0956          -DE/DX =    0.0
!
 ! R27   R(14,74)                1.0998          -DE/DX =    0.0
!
 ! R28   R(15,75)                1.095           -DE/DX =    0.0
!
 ! R29   R(15,76)                1.096           -DE/DX =    0.0
!
 ! R30   R(15,77)                1.0969          -DE/DX =    0.0
!
 ! R31   R(16,78)                1.0953          -DE/DX =    0.0
!
 ! R32   R(16,79)                1.0973          -DE/DX =    0.0
!
 ! R33   R(16,133)               1.0963          -DE/DX =    0.0
!
 ! R34   R(17,18)                1.5522          -DE/DX =    0.0
!
 ! R35   R(17,80)                1.0948          -DE/DX =    0.0
!
 ! R36   R(17,81)                1.0948          -DE/DX =    0.0
!
 ! R37   R(18,19)                1.5502          -DE/DX =    0.0
!
 ! R38   R(18,20)                1.5573          -DE/DX =    0.0
!
 ! R39   R(18,82)                1.1001          -DE/DX =    0.0
!
 ! R40   R(19,83)                1.1014          -DE/DX =    0.0
!
 ! R41   R(19,136)               1.1007          -DE/DX =    0.0
!
 ! R42   R(19,137)               1.5365          -DE/DX =    0.0
!
 ! R43   R(20,21)                1.5389          -DE/DX =    0.0
!
 ! R44   R(20,84)                1.0956          -DE/DX =    0.0
!
 ! R45   R(20,85)                1.0998          -DE/DX =    0.0
!
 ! R46   R(21,86)                1.0953          -DE/DX =    0.0
!
 ! R47   R(21,87)                1.0973          -DE/DX =    0.0
!
 ! R48   R(21,88)                1.0963          -DE/DX =    0.0
!
 ! R49   R(22,27)                1.3931          -DE/DX =    0.0
!
 ! R50   R(22,144)               1.9361          -DE/DX =    0.0
!
 ! R51   R(23,24)                1.3931          -DE/DX =    0.0
!
```

```
 ! R52   R(23,141)               1.9361          -DE/DX =    0.0
!
 ! R53   R(24,25)                1.4078          -DE/DX =    0.0
!
 ! R54   R(24,89)                1.0778          -DE/DX =    0.0
!
 ! R55   R(25,26)                1.3883          -DE/DX =    0.0
!
 ! R56   R(25,90)                1.0826          -DE/DX =    0.0
!
 ! R57   R(26,30)                1.3901          -DE/DX =    0.0
!
 ! R58   R(26,141)               1.9187          -DE/DX =    0.0
!
 ! R59   R(27,28)                1.4078          -DE/DX =    0.0
!
 ! R60   R(27,91)                1.0778          -DE/DX =    0.0
!
 ! R61   R(28,29)                1.3883          -DE/DX =    0.0
!
 ! R62   R(28,92)                1.0826          -DE/DX =    0.0
!
 ! R63   R(29,31)                1.3901          -DE/DX =    0.0
!
 ! R64   R(29,144)               1.9187          -DE/DX =    0.0
!
 ! R65   R(30,32)                1.2277          -DE/DX =    0.0
!
 ! R66   R(31,33)                1.2277          -DE/DX =    0.0
!
 ! R67   R(32,35)                1.3913          -DE/DX =    0.0
!
 ! R68   R(33,34)                1.3913          -DE/DX =    0.0
!
 ! R69   R(34,42)                1.3938          -DE/DX =    0.0
!
 ! R70   R(34,142)               1.8141          -DE/DX =    0.0
!
 ! R71   R(35,36)                1.8141          -DE/DX =    0.0
!
 ! R72   R(35,39)                1.3938          -DE/DX =    0.0
!
 ! R73   R(36,37)                1.8199          -DE/DX =    0.0
!
 ! R74   R(37,38)                1.3994          -DE/DX =    0.0
!
 ! R75   R(37,44)                1.4217          -DE/DX =    0.0
!
 ! R76   R(38,39)                1.4287          -DE/DX =    0.0
!
 ! R77   R(38,61)                1.5145          -DE/DX =    0.0
!
 ! R78   R(39,63)                1.5128          -DE/DX =    0.0
!
 ! R79   R(40,41)                1.3994          -DE/DX =    0.0
!
```

```
 ! R80    R(40,43)                  1.4217          -DE/DX =     0.0
!
 ! R81    R(40,142)                 1.8199          -DE/DX =     0.0
!
 ! R82    R(41,42)                  1.4287          -DE/DX =     0.0
!
 ! R83    R(41,65)                  1.5145          -DE/DX =     0.0
!
 ! R84    R(42,67)                  1.5128          -DE/DX =     0.0
!
 ! R85    R(43,46)                  1.3613          -DE/DX =     0.0
!
```

6. Absorption spectra

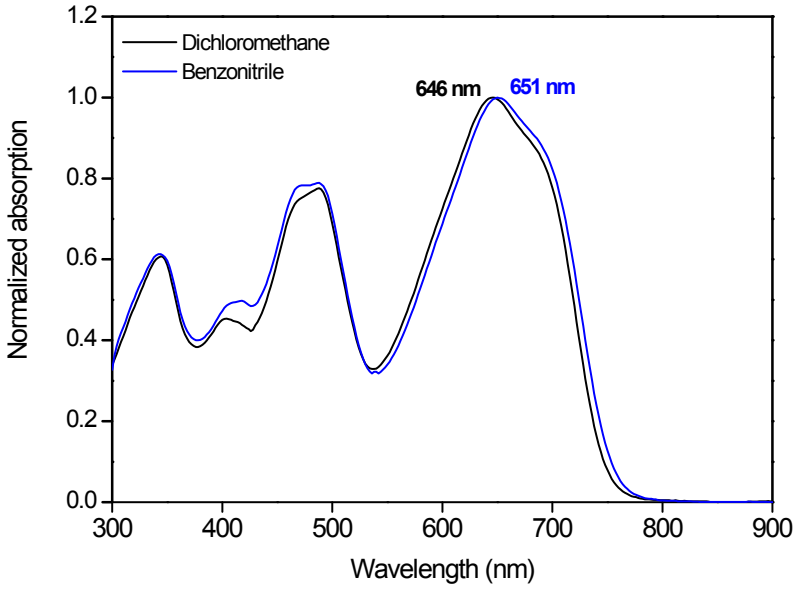

Figure S16. Absorption spectra in solvents with different polarities: dichloromethane and benzonitrile

7. Electrochemical Studies

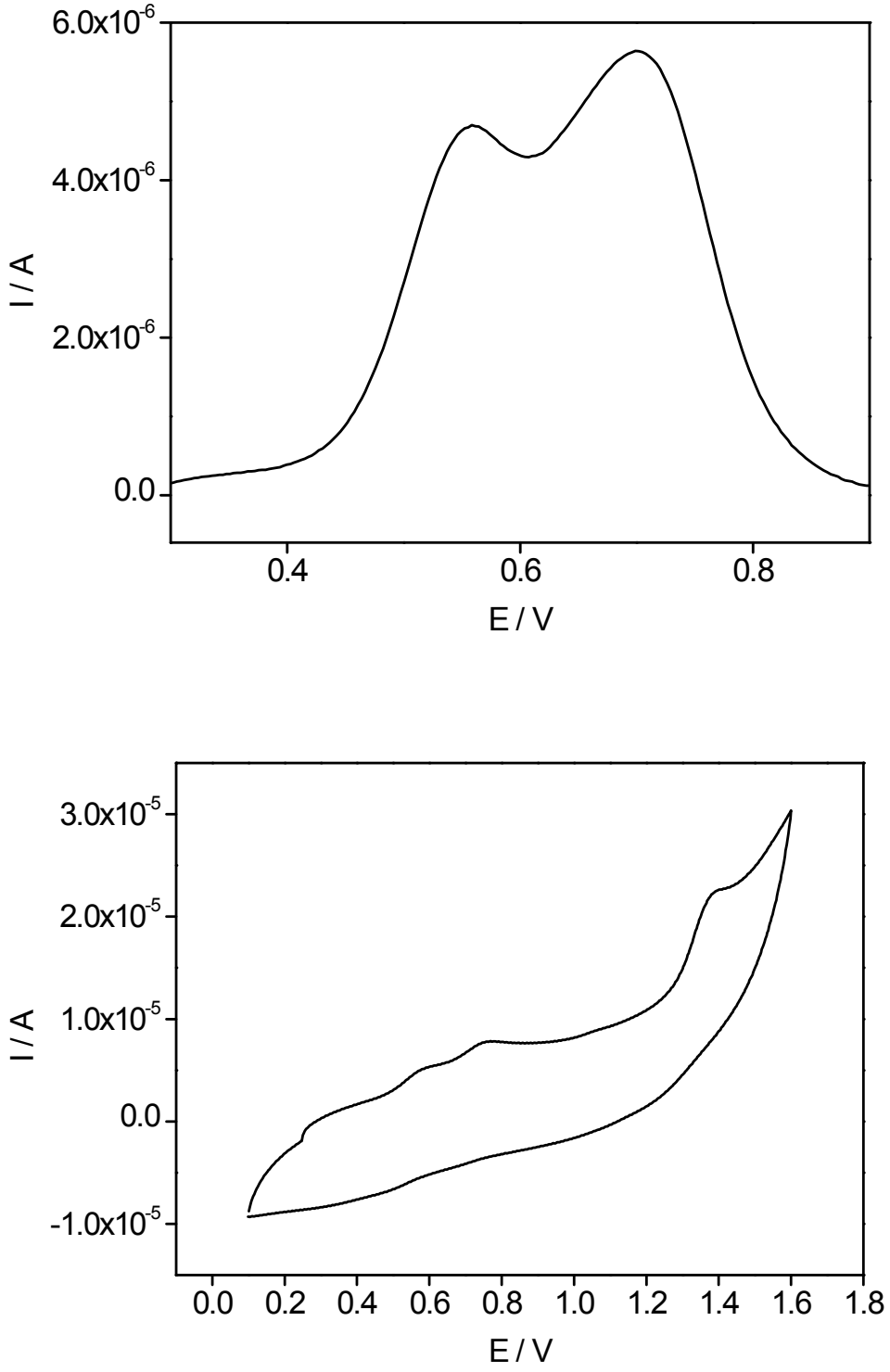

Figure S17. Oxidation side of voltammetries of **MPU6**: Osteryoung square wave (top) and cyclic voltammetry (bottom).

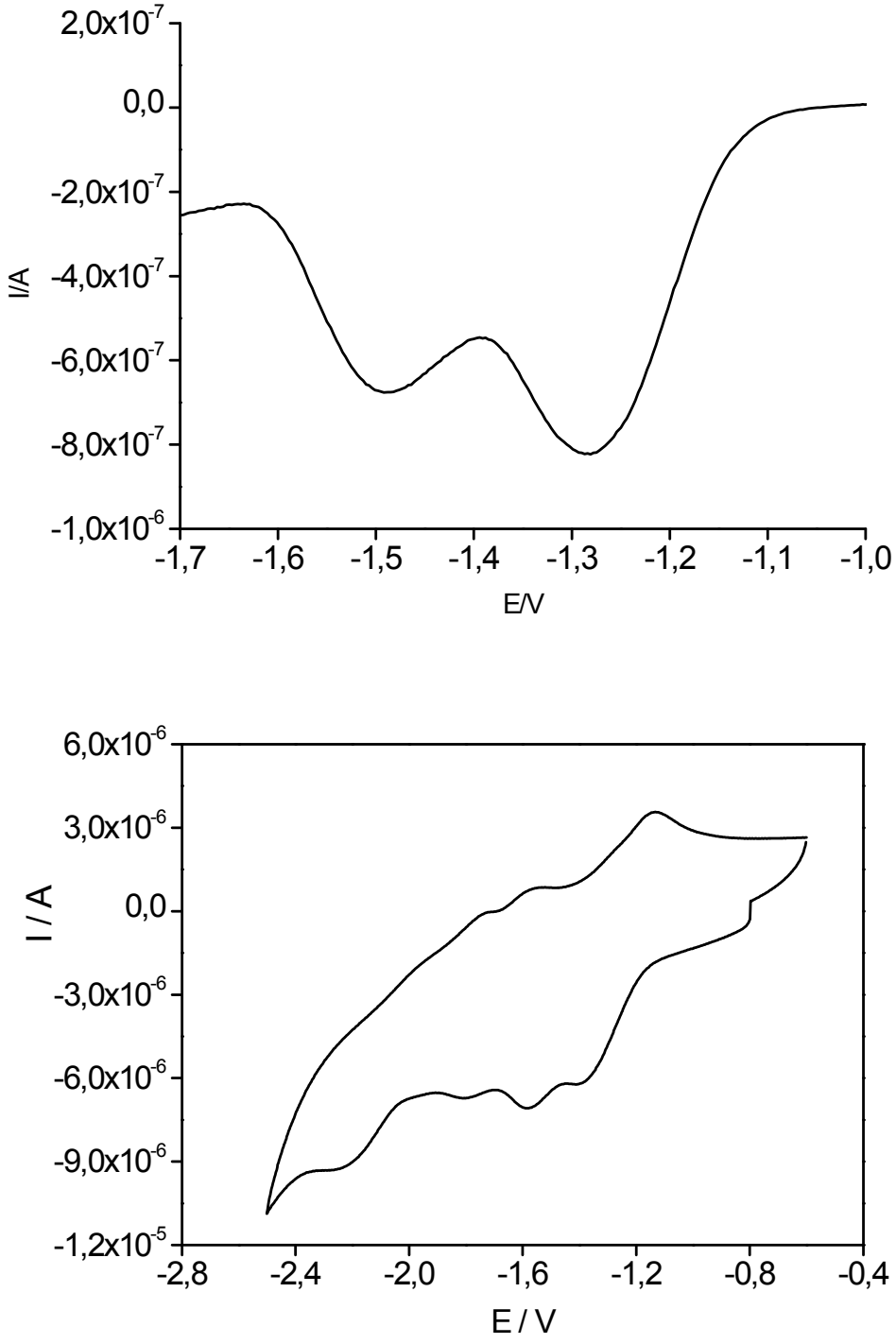

Figure S18. Reduction side of voltammetries of **MPU6:** Osteryoung square wave (top) and cyclic voltammetry (bottom).

8. Photovoltaic Studies

Experimental details for the device fabrication

The solution processed BHJ PSCs were fabricated with a conventional device structure of indium tin oxide (ITO)/PEDOT:PSS (40 nm)/active layer/PFN (20 nm)/Al (50 nm) and fabrication details is as follow: ITO coated glass substrates were cleaned before the device fabrication in acetone, detergent, deionized water, isopropyl alcohol in ultrasonic bath, sequentially and then dried in vacuum oven. A thin film of PEDOT:PSS was spin-casted on the ITO coated glass substrates at 3000 rpm for 30 min and then thermally annealed at 120° C for 30 m. The binary and ternary active layers were prepared from the donor (TDTBTA) and acceptors ($PC_{71}BM$ or **MPU6**) with an overall concentration of 14 mg/mL and then spin cast on the top of the PEDOT:PSS film and then dried. To prepare the ternary active layers, the weight ratios between two acceptors ($PC_{71}BM$ and **MPU6**) are varied keeping the concentration of donor (TDTBTA) constant. The solvent vapor annealing (SVA) treatment was carried out via exposing the active layer in THF environment for 40s. To this end, 2 mL of THF was added into the glass petri dish and then, closed and saturated with solvent vapours for 4 minutes. The as cast film attached on the back side of the second lid was quickly swapped and the lid covering the solvent containing dish. After the SVA exposure the films were removed from the petri dish and were allowed to dry at room temperature for 1 minute. The thickness of the films was about 90 ±5 nm. A thin film of PFN in methanol solution (0.1mg/mL) was spin coated on the top of active layer to form the ETL and then dried. Finally, thin film of aluminium (Al) was thermally deposited on the top of PFN at pressure less than 1×10^{-5} torr with a shadow mask as top electrode. The effective area of the devices was 0.16 cm^2.

The power conversion efficiencies of the devices were determined from the current-voltage characteristics measured by Keithley 2400 source meter unit under AM1.5G, 100 mW/cm^2) spectrum from a solar simulator. The incident photon to current conversion efficiency (IPCE) spectra of the PSCs were recorded using Bentham IPCE system (model 300).

The hole mobility and electron mobility of the blended films were estimated by recording the under dark J-V characteristics of hole only (ITO/PEDOT:PSS/active layer/Al) and electron only (ITO/Al/active layer/Al) and fitting the data with the space charge limited current (SCLC) model.

The transmission electron microscope (TEM) images were recorded on TEM equipment (FEI- Tecnai G^2 F20 S model) using 200 KV field emission gun. The x-ray diffraction patterns of thin films were recorded on PANalytical X'Pert Pro X-ray diffractometer equipped with a CuKα source.

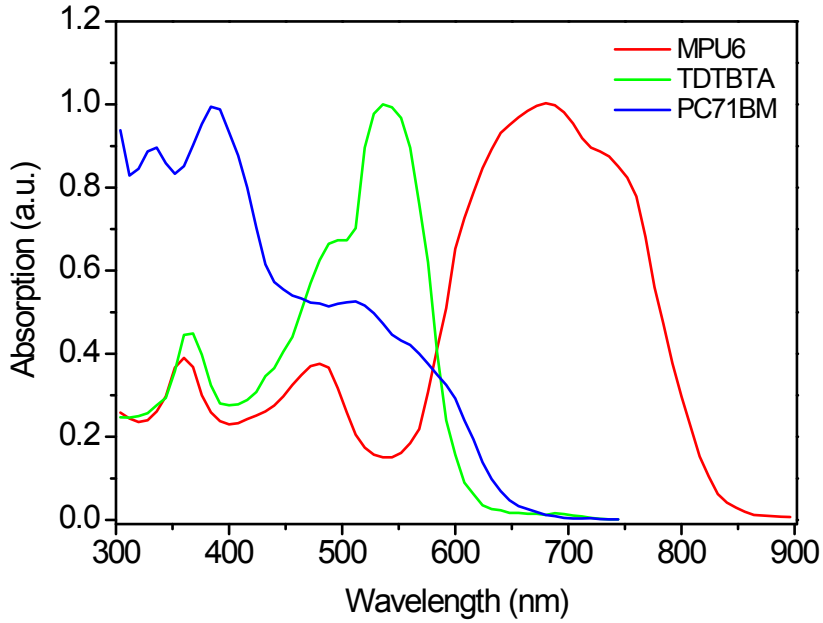

Figure S19. Thin film absorption spectra of TDTBTA (green line), **MPU6** (red line) and $PC_{71}BM$ (blue line); cast from chloroform.

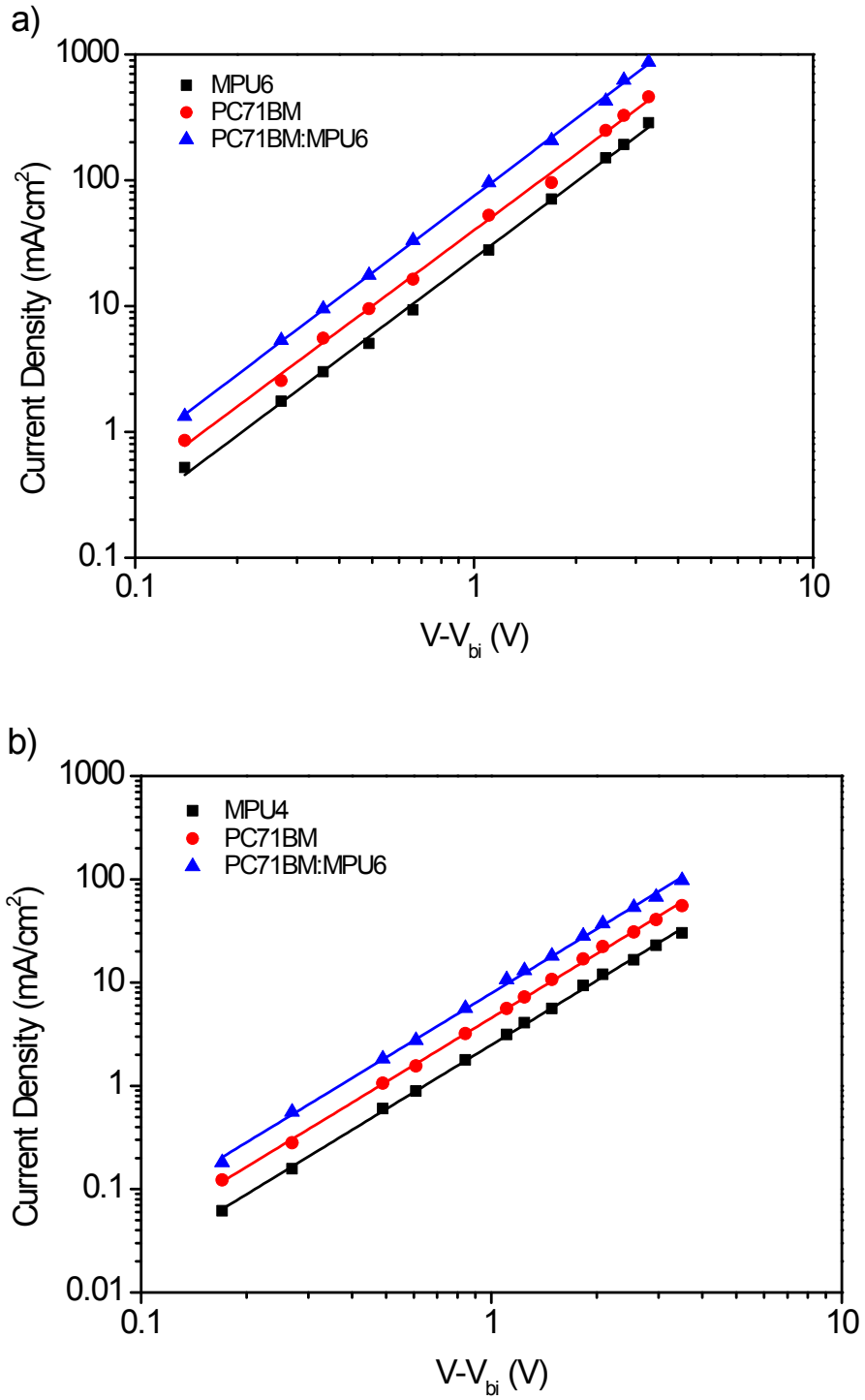

Figure S20. Dark J-V characteristics for (a) hole only and (b) electron only devices.

Table S1(a). Photovoltaic parameters of PSCs based on TDTBTA:**MPU6** with different weight ratios processed with chloroform.

Weight ratio TDTBTA: **MPU6**	J_{SC} (mA/cm^2)	V_{OC} (V)	FF	PCE (%)
1:0.2	12.76	1.07	0.46	6.28
1:0.4	14.06	1.09	0.48	7.36
1:0.8	15.65	1.07	0.50	8.37
1:1.2	16.24	1.08	0.51	8.95
1:1.4	15.02	1.08	0.48	7.79

Table S1(b). Photovoltaic parameters of PSCs based on TDTBTA:$PC_{71}BM$ with different weight ratios processed with chloroform.

Weight ratio TDTBTA:$PC_{71}BM$	J_{SC} (mA/cm^2)	V_{OC}(V)	FF	PCE (%)
1:0.4	6.96	0.96	0.51	3.38
1:0.8	7.12	0.94	0.52	3.80
1:1.2	7.94	0.94	0.53	3.95
1:1.5	8.32	0.95	0.55	4.35
1:1.7	7.89	0.96	0.53	4.01

Table S2(a). Photovoltaic parameters of PSCs based on TDTBTA:**MPU6** (1:1.2) exposed to SVA treatment for different times processed under THF environment.

SVA time	J_{SC} (mA/cm^2)	V_{OC}(V)	FF	PCE (%)
10 s	17.97	1.07	0.57	10.96
20 s	19.34	1.06	0.59	12.28
40 s	20.38	1.04	0.62	13.14
50 s	19.56	1.02	0.60	11.97

Table S2(b) Photovoltaic parameters of PSCs based on TDTBTA:$PC_{71}BM$ (1:1.2) exposed to SVA treatment for different times processed under THF environment.

SVA time	J_{SC} (mA/cm^2)	V_{OC}(V)	FF	PCE (%)
10 s	9.34	0.92	0.59	5.07
20 s	10.75	0.91	0.64	6.26
40 s	11.22	0.89	0.67	6.69
50 s	10.76	0.87	0.65	6.08

Table S3(a). Photovoltaic parameters of PSCs based on TDTBTA:$PC_{71}BM$:**MPU6** with different weight ratios processed with chloroform.

TDTBTA: $PC_{71}BM$:**MPU6**	J_{SC} (mA/cm^2)	V_{OC}(V)	FF	PCE (%)
1:0.1:1.1	16.87	0.99	0.55	9.18
1:0.2:1.0	17.78	0.99	0.58	10.21
1:0.3:0.9	18.27	1.00	0.62	11.32
1:0.4:0.8	17.67	1.01	0.59	10.53

Table S3(b) Photovoltaic parameters of PSCs based on TDTBTA:$PC_{71}BM$:**MPU6** (1:0.3:0.9) under SVA treatment for different times.

SVA time	J_{SC} (mA/cm^2)	V_{OC}(V)	FF	PCE (%)
10 s	19.54	0.96	0.66	12.38
20 s	21.98	0.96	0.69	14.56
40 s	22.65	0.97	0.71	15.60
50 s	21.72	0.95	0.69	14.24